

## Depinar, a drug that potentially inhibits the binding and entry of COVID-19 into host cells based on computer-aided studies

Meysam Yazdani<sup>1</sup>, Jafar Khezri<sup>1</sup>, Nastaran Hadizadeh<sup>2</sup>, Javad Zamani Amir Zakaria<sup>3</sup>, Mousa Naderi<sup>1</sup>, Sahar Mahmoodian<sup>3</sup>, Ali Asghar Karkhanei<sup>1</sup>, Farideh Razi<sup>4</sup>, Mohammad Hossein Sanati<sup>5,\*</sup>, and Ehsan Hashemi<sup>2,6,\*</sup>

<sup>1</sup>Department of Systems Biotechnology, Institute of Industrial and Environmental Biotechnology, National Institute of Genetic Engineering and Biotechnology (NIGEB), Tehran, I.R. Iran.

<sup>2</sup>Diabetes Research Center, Endocrinology and Metabolism Clinical Sciences Institute, Tehran University of Medical Sciences, Tehran, I.R. Iran.

<sup>3</sup>Department of Animal Biotechnology, National Institute of Genetic Engineering and Biotechnology, Tehran, I.R. Iran.

<sup>4</sup>Endocrinology and Metabolism Research Center, Endocrinology and Metabolism Clinical Sciences Institute, Tehran University of Medical Sciences, Tehran, I.R. Iran.

<sup>5</sup>Medical Genetics Department, National Institute of Genetic Engineering and Biotechnology, Tehran, I.R. Iran.

<sup>6</sup>National Research Centre for Transgenic Mouse, National Institute of Genetic Engineering and Biotechnology, Tehran, I.R. Iran.

### Abstract

**Background and purpose:** The new coronavirus (Covid-19) has resulted in great global concerns. Due to the mortality of this virus, scientists from all over the world have been trying to employ different strategies to tackle down this concern. This virus enters cells *via* phagocytosis through binding to the angiotensin-converting enzyme II receptor. After invading the body, it can stay hidden in there for a period of up to 24 days (incubation period).

**Experimental approach:** In this report, by the use of *in silico* studies we selected several FDA-approved compounds that possess antiviral properties. We chose the viral Spike protein as the target of drug compounds and carried out the screening process for the FDA databank in order to find the most effective ligand.

**Findings/Results:** The results from dock and MD revealed 10 compounds with high affinity to the receptor-binding domain motif of S protein. The best inhibitors were the ingredients of Depinar, which managed to effectively block the interactions between cells and virus.

**Conclusion and implication:** The results of this study were approved by *in silico* studies and due to the lack of time; we did not test the efficiency of these compounds through *in vitro* and *in vivo* studies. However, the selected compounds are all FDA approved and some are supplements like vitamin B12 and don't cause any side effects for patients.

**Keywords:** Corona; Covid-19; Depinar; Docking-based virtual screening; Molecular dynamics.

### INTRODUCTION

Sars-Cov-2 virus was initially detected in Hubei Province, China toward the end of the year 2019 and is currently spreading dramatically in many other countries (1). Due to the lack of effective clinically approved drugs, its fast regeneration rates, and its lethality listed among public health life-threatening factors by the World Health Organization (WHO). This virus is a member of

the Coronaviridae family, which are membrane-coated RNA viruses that mostly attack the respiratory systems of birds and mammals (2). Unlike the influenza virus that has a multi-segmented genome (3), the Corona virus's genome is single-stranded and contiguous (4).

#### Access this article online



Website: <http://rps.mui.ac.ir>

DOI: 10.4103/1735-5362.314830

\*Corresponding authors:

E. Hashemi, Tel: +98-88631298, Fax: +98-88220052

Email: E\_hashemi@nigeb.ac.ir

H. Sanati, Tel: +98-2144787301, Fax: +98-2144787399

Email: M-sanati@nigeb.ac.ir

After binding to angiotensin-converting enzyme II (ACE2) receptor, the virus enters the cell *via* endocytosis (5). Toward entering the body, it can stay hidden for a period of up to 24 days (incubation period). After an incubation period, most patients show weak clinical symptoms and therefore won't need medical care. However, in others, symptoms usually start in one week followed by the invasion of this virus to the body. Patients might experience fever, coughs, nasal congestion, exhaustion, hard breathing, and in some cases severe chest symptoms corresponding to pneumonia (6-8). Sars-Cov-2 virus is less lethal than other pathogenic viruses in the same family. SARS and MERS mortality rates are 9.6% and 34.4% among infected patients, respectively (9-11). However, Sars-Cov-2 virus mortality rate is estimated at 2.3% (in China), but its total death was higher than SARS and MERS in few months after virus detection (12).

While this virus has disrupted the lives of people in many countries, spreads out incredibly fast, and threatens the lives of many in different places, however, there is not enough time to design, examine, and mass produce a new drug against this virus. The discovery and industrial production of a new drug usually takes a few years (13-15). Furthermore, producing and carrying out a vaccination process might also take a few months (16). Therefore, screening existing drugs for finding possibly effective medicine that can be used for the treatment of Covid-19 infection is of significant importance. Moreover, it has often occurred that a drug designed for the treatment of a certain disease, has shown good therapeutic effects for the treatment of another disease (in some cases because of target homology or similar disease mechanism) (17). This phenomenon happens with the discovery of a new application for a previously used drug and is called drug repositioning (18). This study was constructed to identify inhibitory compounds with medicinal potential against Sars-Cov-2 virus. The viral Spike protein was chosen as the target of drug compounds (19,20). This protein plays a key role in the binding of Sars-Cov-2 virus to cell receptors and integration of the virus with the cell membrane (21). Spike is a trimer protein that has different functional parts. An important priority of ours in this study

was the prevention of this virus from binding to receptors in human host cells. A part of the S1 domain, known as the receptor-binding domain (RBD), is in charge of receptor binding. This domain in Sars-Cov-2 has widely mutated from that of Sars-Cov virus and these differences have caused higher binding affinity to human ACE2 receptor (22). Inhibiting this domain of Spike protein can probably prevent binding and subsequently cell insertion of this virus, or slow down its reproduction cycle.

## MATERIALS AND METHODS

### *Protein preparation*

Crystallographic structure of the Spike protein was recently published with 3.5Å resolution and with the PDB code of 6VSB (1). RBD domain in Covid-19 virus consists of 183 amino acids and according to the reported crystallographic structure; it has a few gaps that can play major roles in different interactions and also in how the virus binds to its human cell receptors. Therefore, due to the existence of gaps between amino acids in RBD, loop refinement was carried out using modeler version 9.11, all the while taking the FASTA sequence of the main protein and structures of other monomers of this protein, into consideration. Some changes were made in the crystallographic structure and then for approving the stereochemical structure, volume, area, dihedral angle reporter (VADAR) server was employed for checking the volume, areas, and dihedral angle reporters.

For obtaining the 3D structure of the ACE2 receptor; chain "A" of the PDB structure of SARS coronavirus's Spike protein's receptor-binding complex (2AJF) was extracted. Both PDB structures were obtained from the protein databank (<http://www.rcsb.org>), and co-crystallized ligands, water molecules, and ions were removed from the structures.

### *RBD binding (interface) site detection*

For predicting all possible interactions between this viral protein and its human cell receptors that are responsible for virus binding and subsequent membrane fusion, the refined RBD of 3D crystallographic structures of SARS Spike protein and "A" chain of ACE2 complex were selected (2AJF). The S trimer

protein has two domains and different areas. Our priority in this study was preventing this virus from binding to receptors in human epithelial cells which is taking place through a part of the S1 domain known as RBD. This area in Covid-19 has some differences from that of SARS virus and these differences have caused the corona virus's higher binding affinity toward human ACE2 receptors. Inhibiting this part of the Spike protein can probably prevent the fusion and subsequently lethality of this virus. Prior to carrying out the virtual screening process, HADDOCK 2.2 (high ambiguity-driven biomolecular docking) was employed to identify the best conformational position for RBD binding site to ACE2 receptor. Key amino acids involved in the interaction between these two proteins were identified based on ACE2-SARS coronavirus Spike protein complex.

### Ligand's library

Given the current condition and extreme urgency for finding possible treatments, virtual screening was carried out for FDA-approved drugs. A 3D FDA library containing more than 1400 drugs was chosen and their 3D structures were obtained from BD data bank databases in SDF format.

### Virtual screening and docking

A free version of Molegro Virtual Docker (MVD) was used for predicting protein-drug interactions. The ligand-to-protein binding site of RBD was obtained from the results of HADDOCK2.2. Before the virtual screening process, proteins and ligand libraries were energy minimized. Virtual screening was carried out using the MolDock SE algorithm and MolDock scoring functions.

### Molecular dynamics simulation

Molecular dynamics techniques were applied to evaluate the stability of the protein-ligand complex utilizing GROMACS 4.6.5 software package. The GROMOS 54A7 force field was used to create proper topologies. The complexes were placed at the center of a cubic box and solvated with the TIP3P water model. 4  $\text{Cl}^+$  ions were used for neutralizing the system. The solvated-neutralized system was subjected to energy minimization with 5000 steps to remove all short contacts using the steepest descent algorithm. Subsequently, the equilibration of systems was done under NVT and NPT at a temperature of 300 K and pressure of 1 bar, respectively, with restraint forces of 1000 kJ/mol.

The electrostatic interactions were calculated using the Particle Mesh Ewald (PME) method. Finally, a 40 ns molecular dynamics (MD) run with no restraints was performed for evaluating the stability of the protein-drug complex. Also, MD trajectory data were used to calculate the binding free energy of protein-inhibitor complex using g-mmpbsa tool of molecular mechanics Poisson-Boltzmann surface area (MM-PBSA).

## RESULTS

### Refined RBD evaluation

After the loop refinement using modeler software, the new structure must be evaluated and confirmed. We used VADAR and ProSA web tools for the reliability of the new structure. The -4.95 Z-score predicted by ProSA indicates the good quality of the model (Fig. 1A).

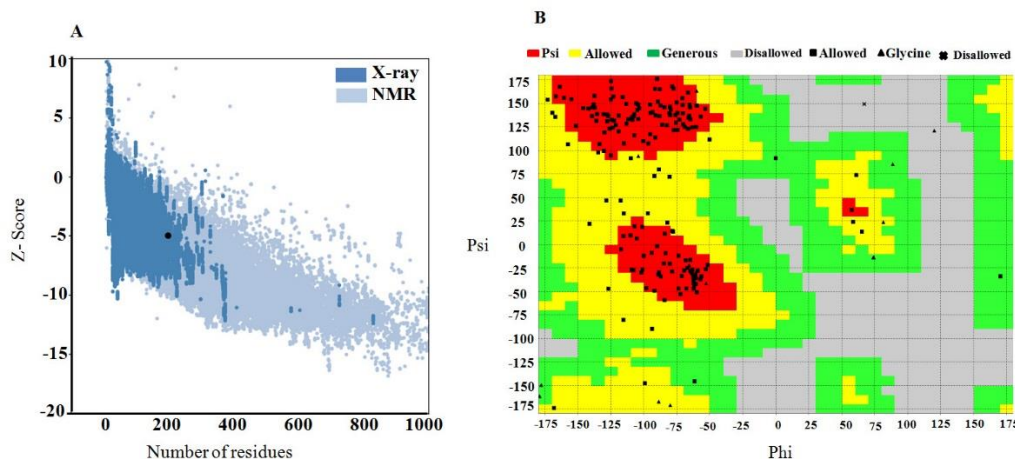


**Fig. 1.** Overall quality and quantity checking of refined receptor-binding domain structure, (A) z score from PROSA web server and (B) Ramachandran plot generated using VADAR server.

In addition to showing the quality of the model, the Z score also measures the total energy divergence of the structure with respect to the energy distribution obtained from random conformations. Ramachandran plot obtained from VADAR represents the positions of refined RBD amino acids (Fig. 1B). Most amino acids were plotted in the core region and only one amino acid present in the disallowed region (Fig. 1B and Table 1). The  $\alpha$ -helix,  $\beta$ -sheet, and coil in the refined RBD subdomain of S protein obtained from the modeler were

7%, 30%, and 61%, respectively. The total volume was 25805.8 Å<sup>3</sup>, while the expected volume was estimated to be 25981.6 Å<sup>3</sup>. The accessible surface area (ASA) was measured in the fractional ASA range of 0 to 1 and the results indicated that a large part of the structure is hydrophobic (Table 2 and Fig. 2A). The plots of fractional residue volume, 3D profile quality, stereo/packing quality index in Fig. 2, and orientation of dihedral angles are given in Table 3.

**Table 1.** Resolution values assessment of refined receptor-binding domain structure.

Statistics	Resolution values	
	Observed Å <sup>2</sup>	Expected Å <sup>2</sup>
res in pipsi core	163 (84%)	174 (90%)
res in pipsi allowed	27 (13%)	14 (7%)
res in pipsi generous	2 (1%)	2 (1%)
res in pipsi outside	1 (0%)	0 (0%)
res in omega core	185 (95%)	185 (96%)
res in omega allowed	6 (3%)	6 (3%)
res in omega generous	0 (0%)	0 (0%)
res in omega outside	2 (1%)	2 (1%)
packing defects	13	13
Free energy of folding	-177.47	-175.05
res 95% buried	43	53
Buried charges	0	0

**Table 2.** Accessible surface area computed in refined receptor-binding domain structure using VADAR server.

Statistics	Accessible surface area (ASA)	
	Observed Å <sup>2</sup>	Expected Å <sup>2</sup>
Total ASA	10189.6 Angs**2	9235.6 Angs**2
ASA of backbone	1257.7 Angs**2	-
ASA of sidechains	8931.8 Angs**2	-
ASA of C	6144.0 Angs**2	-
ASA of N	804.2 Angs**2	-
ASA of N+	454.3 Angs**2	-
ASA of O	2347.3 Angs**2	-
ASA of O-	363.5 Angs**2	-
ASA of S	76.2 Angs**2	-
Exposed nonpolar ASA	6107.3 Angs**2	6215.6 Angs**2
Exposed polar ASA	2868.7 Angs**2	2037.9 Angs**2
Exposed charged ASA	1213.6 Angs**2	1936.0 Angs**2
Side exposed nonpolar ASA	6081.7 Angs**2	-
Side exposed polar ASA	1686.7 Angs**2	-
Side exposed charged ASA	1163.4 Angs**2	-
Fraction nonpolar ASA	0.60	0.61 sd=0.03
Fraction polar ASA	0.28	0.20 sd=0.05
Fraction charged ASA	0.12	0.19 sd=0.05
Mean residue ASA	52.8 sd=46.3	-
Mean frac ASA	0.3 sd=0.3	-
side ASA hydrophobic	27.82	-

VADAR, Volume, area, dihedral angle reporter.

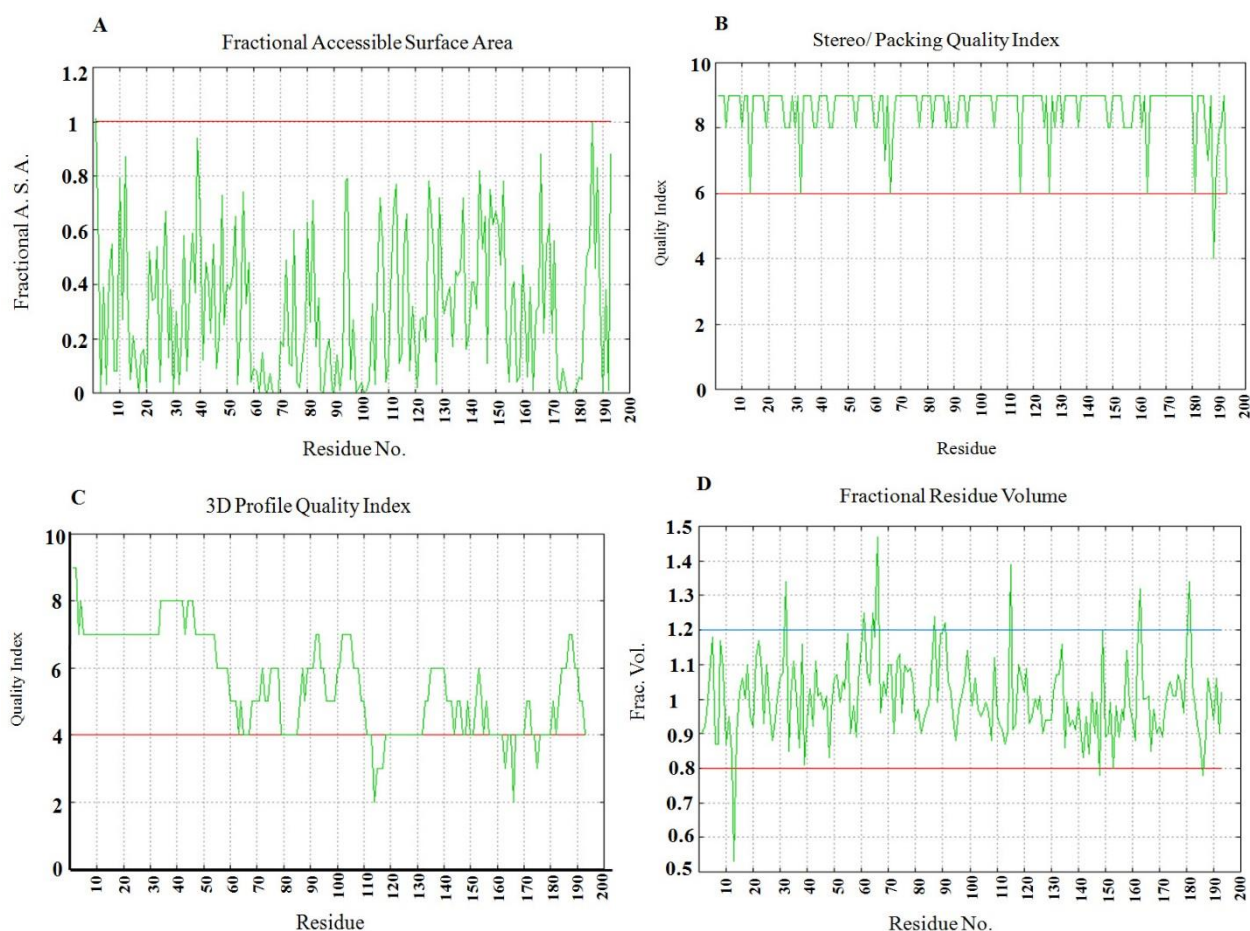


**Fig. 2.** Analysis of refined receptor-binding domain using VADAR server. Plotted estimation results of (A) fractional accessible surface area data, (B) stereo/packing quality index, (C) 3D profile quality index, and (D) fractional residue volume. VADAR, Volume, area, dihedral angle reporter.

**Table 3.** Dihedral Angle reports of refined receptor-binding domain structure calculated by VADAR server.

Statistics	Dihedral angles	
	Observed $\text{\AA}^2$	Expected $\text{\AA}^2$
Mean Helix Phi	$-74.7 \pm 16.4$	$-65.3 \pm 11.9$
Mean Helix Psi	$-42.9 \pm 37.6$	$-39.4 \pm 25.5$
res with Gauche+ Chi	79(50%)	85(55%)
res with Gauche- Chi	28(17%)	31(20%)
res with Trans Chi	49(31%)	39(25%)
Mean Chi Gauche+	$-64.3 \pm 17.2$	$-66.7 \pm 15.0$
Mean Chi Gauche-	$59.5 \pm 15.5$	$64.1 \pm 15.7$
Mean Chi Trans	$167.4 \pm 13.4$	$168.6 \pm 16.8$
Std. dev of Chi pooled	15.70	15.70
Mean omega (omega>90)	$179.7 \pm 4.8$	$180.0 \pm 5.8$
res with omega<90	2(1%)	$180.0 \pm 5.8$

VADAR, Volume, area, dihedral angle reporter.

### HADDOCK

Table 4 shows docking energy values of docking complexes by HADDOCK 2.2. Cluster 5 was considered the best binding pattern according to its scoring functions (Fig. 3). The space around this interface residue and its adjacent residues was considered as the solution space of ligand-protein docking.

### Docking-based virtual screening

Results from molecular docking and virtual screening demonstrated high inhibitory properties in Depinar drug which is a combination of tannic acid and cyanocobalamin. These compounds showed high binding affinities to the RBD domain. For further confirmation of these results, tannic

acid-RBD complex was chosen for dynamic molecular docking and was shown to be highly stable. A list of 10 best compounds obtained from docking results is presented in Table 5 which also mentions their binding affinities. The 2D structure of ligands tannic acid and cyanocobalamin in interaction with the refined RBD residues is shown in Fig. 4.

Different studies have reported the efficiency of tannic acid against various viruses. The suggested compound for the treatment of Covid-19 doesn't need clinical trial phases and is a beneficial compound for the body and testing it on patients under coronavirus infection conditions has no harmful side effects in specified doses.

**Table 4.** Docking energy values of docking complexes using HADDOCK.

Complex	Cluster	HADDOCK score	Cluster size	RMSD	Van der Waals energy	Electrostatic energy	Buried surface area	Z score
1	5	-102.9	10	10.5	-98.4	-554.0	3350.2	-1.8
2	9	-95.6	5	0.6	-109.0	-708.6	3639.4	-1.4
3	1	-82.2	91	15.9	-108.5	-492.4	3318.4	-0.6
4	7	-71.3	7	7.6	-100.4	-437.8	2988.9	-0.0
5	3	-71.1	13	20.0	-108.2	-383.8	3248.7	-0.0
6	8	-70.1	5	20.0	-102.9	-551.1	3069.8	0.1
7	11	-63.8	4	22.4	-97.0	-441.2	3202.6	0.4
8	10	-57.8	4	10.5	-94.8	-555.9	3163.7	0.8
9	4	-48.9	12	18.1	-99.9	-405.1	3088.7	1.3
10	2	-46.9	15	5.8	-111.7	-263.1	3216.1	1.4

**Table 5.** Best results obtained from the docking and virtual screening process and each of their bonding tendencies.

Drugs	Moldock score	Rerank score	H bond
Depinar; tannic acid	-333.421	239.181	-19.2379
Depinar; cyanocobalamin	-277.24	116.354	-15.0319
Eraxis; anidulafungin	-246.308	-67.9741	-5.57019
Oxytocin	-215.519	-101.682	-9.23662
Eptifibatide	-215.181	-102.354	-8.81754
Octreotide acetate	-214.889	-51.1152	-4.48438
Concentraid; desmopressin acetate	-202.624	-66.1945	-5.35674
Marqibo kit; vincristine sulfate	-195.042	-106.219	-2.22595
Ganirelix acetate	-190.619	-51.7166	-7.08877
Kinevac; sincalide	-187.144	-102.308	-7.39883

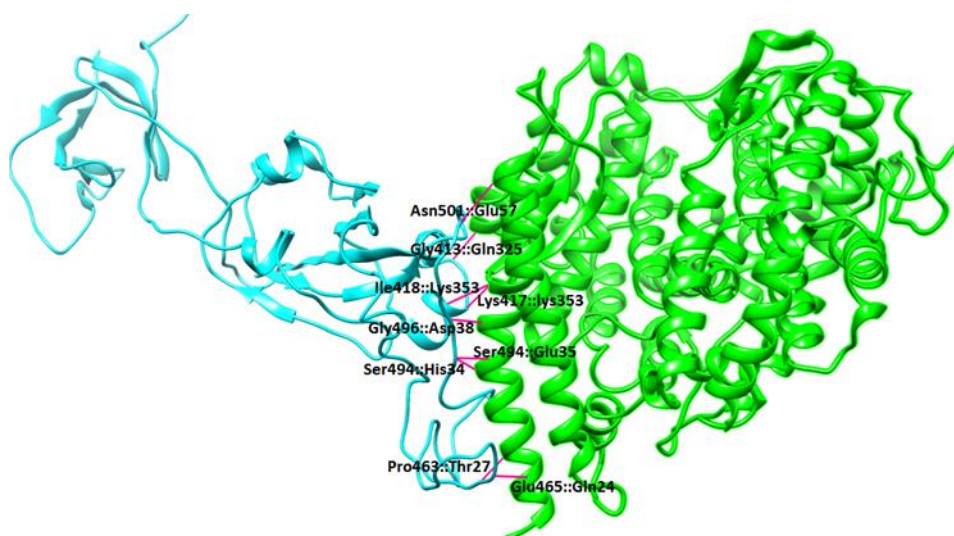


**Fig. 3.** The best-predicted complex suggested by HADDOCK 2.2 and possible interactions between angiotensin-converting enzyme II protein receptor and viral receptor-binding domain. The green color shows the angiotensin-converting enzyme II and blue shows the viral receptor-binding domain.

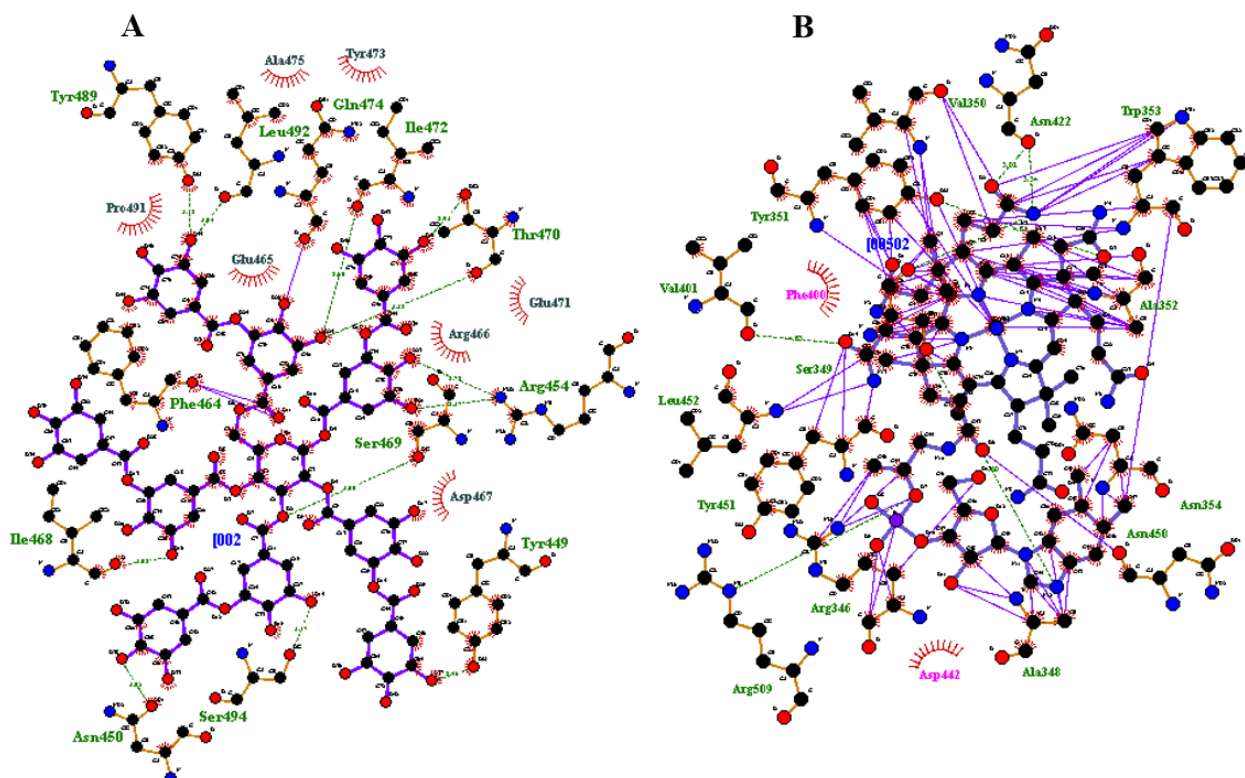


**Fig. 4.** Top scoring drugs tannic acid (A) and cyanocobalamin (B) and their interactions with the refined receptor-binding domain of Covid-19 viral Spike protein. Hydrogen bonds are shown as green dotted lines.

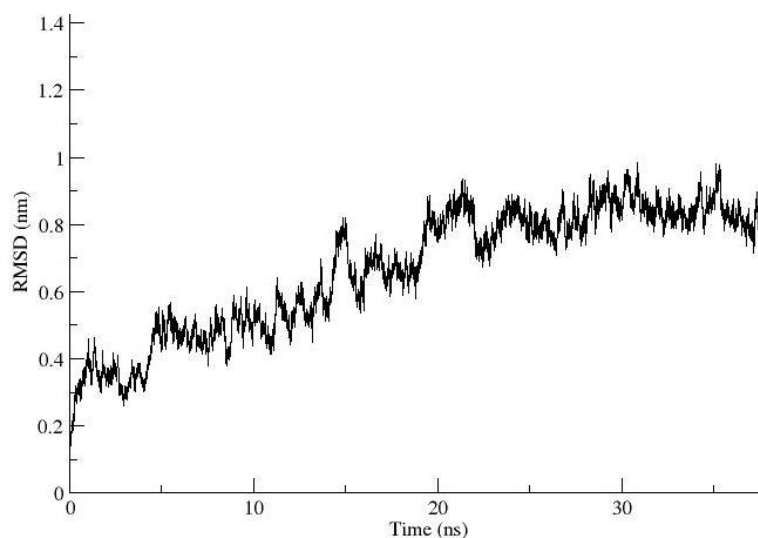


**Fig. 5.** RMSD plot of protein in complex with ligand during 40ns of simulation. As clearly shown, the RMSD value reached about 0.8 nm after 25 ns of simulation and showed no significant fluctuations afterward. RMSD, Root mean square deviation.

#### **Root mean square deviation results**

The backbone root means square deviation (RMSD), which indicates structural stability, is a crucial analysis to evaluate the MD simulations. Therefore, the backbone deviation of protein inbouded from the initial structure

was plotted as a function of time. As shown in Fig. 5 the RMSD value for this protein was in the range of 0.15 to 0.85 nm during simulation. Also, the RMSD value reached 0.8 nm after 25 ns simulation and showed no significant fluctuations afterward.

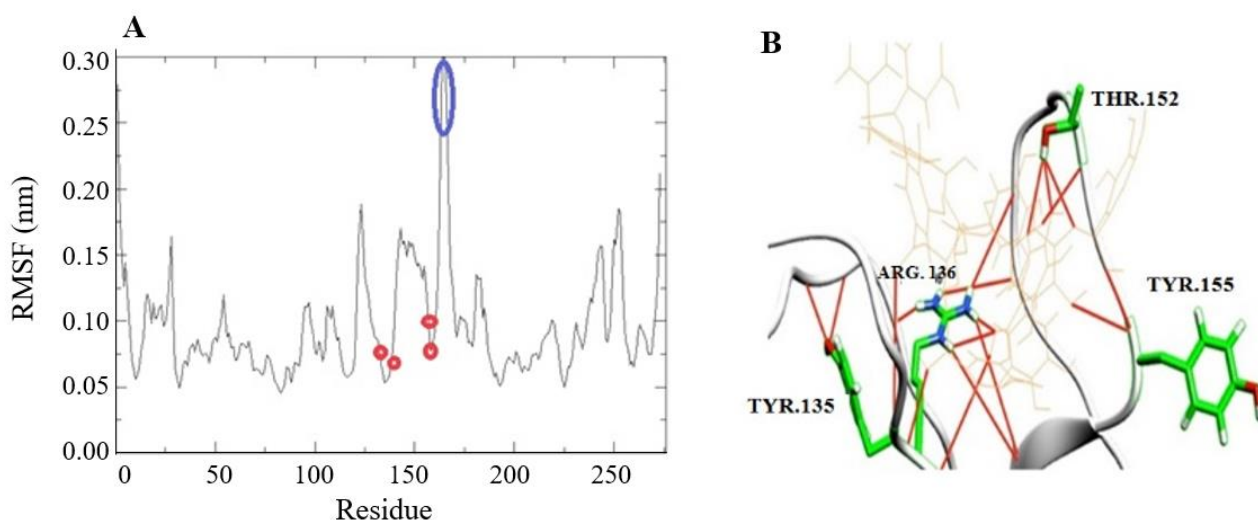


**Fig. 6.** (A) RMSF plot and binding residues of the protein in complex with ligand, the regions highlighted in red show the binding residues with lower RMSF values, and the regions highlighted in blue show residues with higher values located in the loop region. (B) Binding residues are shown in stick forms and ligands are shown in wire forms. RMSF, Root mean square fluctuation.

**Table 6.** MM/PBSA free energies of tannic acid-receptor-binding domain complex calculated from molecular dynamics trajectory data.

Energies (kcal/mol)	
van der Waals energy ( $\Delta E_{VDW}$ )	-218.825
Electrostatic energy ( $\Delta E_{ELE}$ )	-75.581
Polar solvation energy ( $\Delta E_{PBCAL}$ )	136.920
SASA energy ( $\Delta E_{ELE}$ )	-23.782
SAV energy	0.000
WCA energy	0.000
Binding energy	-181.268

### Root mean square fluctuation

We also calculated the root mean square fluctuation (RMSF) of this system. This plot shows flexible regions of this complex and the residues with small degrees of fluctuation are regarded as stable. As indicated in Fig. 6A and B residues involved in interaction with ligand including Tyr 135, Arg 136, Gln 156, and Thr 152 showed significantly lower RMSF values, while the residues located in the loop region showed higher RMSF values. In conclusion, the results showed the stability of this protein-ligand complex.

### MM/PBSA

The binding free energy and its related components calculated through the MM/PBSA method were listed in Table 6. The results indicated that relative binding free energies of the tannic acid-RBD complex supported the

potent binding in the dynamic system. The electrostatic interactions, van der Waals, and SASA energy had a negative effect and only polar solvation energy had a positive effect on total interaction energy.

## DISCUSSION

It appears that Covid-19 has no effective treatment and due to the fast spreading of this virus all around the world and its mortality, the emergency of finding a drug that inhibits virus activity to some extent is pivotal. Up to now, many compounds have been registered to have antiviral activities. Effective drugs must inhibit an enzyme or a functional protein in this virus or even block the path of virus interaction with host cells. Some studies have attempted to either work on antiviral activities or indirectly reduce the disease's symptoms like inflammation. For instance, artificial intelligence suggests that AP2-associated protein kinase 1 inhibiting drug can disrupt the invasion of this virus into cells. Drugs with the potential for preventing cytokine storms such as ALK and suramin inhibitors are possibly effective in preventing the acute and lethal phase of this disease (23). Galidesvir, lopinavir, and ritonavir are drugs that cause disruption in viral polymerase activity and have been suggested for treatment (24). A combination of



anti-retrovirus drugs such as lopinavir and ritonavir has shown positive clinical therapeutic responses in Sars-Cov patients and is probably also effective in treating Covid-19 (25,26). Galidesivir is a viral RNA polymerase inhibitor nucleotide and has shown successful therapeutic effects in lethal viral diseases and can be a possible candidate for treating corona (26).

Due to the fact that S protein plays a central role in virus entrance to host cells, this is an interesting target for drug discovery and virtual screening. The RBD subdomain of S protein is responsible for the initial interaction of virus and host receptor (27). The anti-ACE2 receptor components can inhibit this interaction and subsequently block the entrance of the virus to human cells. But there is no evidence which supports ACE2 receptor is the only receptor for this virus (28). Moreover, the recent reports have nominated CD147 as the other receptor to interact with S protein. Thus, selecting the S protein inhibitor to inhibit the entrance of the virus to the host cell seems more logical. Antiviral drug (Arbidol) with a similar mechanism can inhibit fusion and entrance of the influenza virus to the host cell (29).

Virtual screening processes have been carried out for FDA-approved drugs *via* molecular docking systems intending to find Covid-19 viral Spike inhibitors. A number of possible compounds have been represented, some of which are well-known retrovirus inhibitors (30-32). Some of these compounds that have better binding affinities than inhibitors are designed for retroviruses (like HIV) protease inhibition (33). Also, Prajapat *et al.* suggested potential inhibitors using virtual screening and molecular dynamics of FDA-approved drugs against Spike protein (34). In a similar study, a library of FDA-approved drugs has been docked with papain-like protease (PLpro). A few preferred compounds such as chloroquine and formoterol have been suggested as possible inhibitors of this protease (26). In another similar work, more than 1600 FDA-approved compounds have been docked with the virus's main protease substrate binding site and an antihepatitic drug called Csimeprevir was represented as a possible inhibitor of this virus's main protease (35-36).

In our study, FDA-approved compounds were screened virtually and it was found that Depinar (a drug composed of cyanocobalamin, zinc acetate, and tannic acid) is the best drug for inhibition of virus RBD domain and ACE2 receptor interactions.

Clinical trial studies revealed vitamin B<sub>12</sub> supplementation could significantly improve responses to antiviral therapy in patients infected with hepatitis C virus (37). Moreover, low levels of vitamin B<sub>12</sub> and its malabsorption were detected in HIV patients along with gastrointestinal symptoms (38).

Another component of Depinar drug; zinc as a crucial micronutrient regulates diverse biological functions and has been shown to have antiviral properties. Zinc has an important role in the replication of many viruses, and the antiviral action of this compound was previously reported as it can inhibit replication in viruses, moreover, Zn<sup>2+</sup> can interfere with some of the replicase enzyme's polyprotein cleavages (39,40). Our results suggested Depinar as the best inhibitor for RBD and ACE2 receptor interactions and docking results revealed either Depinar alone or its components cyanocobalamin and tannic acid have high binding affinities to RBD domain of the S protein. Previous researches have revealed that zinc can inhibit virus activity through binding to RNA polymerase of the virus.

## CONCLUSION

The results of this *in silico* study suggest that Depinar, a complex drug composed of tannic acid, cyanocobalamin, and zinc acetate can effectively bind to the Spike protein of Sars-Cov-19 and probably block the RBD and ACE2 receptor interactions. This activity can inhibit the invasion of the virus to cells and consequently block the virus reproduction cycle; therefore, this compound may act as a potent antiviral drug for the treatment of coronavirus infection

## Acknowledgments

The study was financially supported by Tehran University of Medical Sciences under Grant No. 1399-01-97-993. The authors would like to thank the Research Council at the National

Institute of Genetic Engineering and Biotechnology and Tehran University of Medical Sciences for their support and provision of facilities.

### Conflict of interest statement

The authors declared no conflict of interest for this study.

### Authors' contribution

M. Yazdani and J. Zamani Amir Zakaria contributed to the experimental studies and data analysis; J. Khezri, concept and data analysis; N. Hadizadeh and F. Razi prepared and edited the manuscript; M. Naderi and S. Mahmoodian carried out the experimental studies; A.A. Karkhanei acquired and analyzed the data; M.H. Sanati contributed in concept, and E. Hashemi contributed in concept and manuscript preparation and editing.

## REFERENCES

1. Wu Z, McGoogan JM. Characteristics of and important lessons from the coronavirus disease 2019 (COVID-19) outbreak in China: summary of a report of 72 314 cases from the Chinese Center for Disease Control and Prevention. *JAMA*. 2020;323(13):1239-1242. DOI:10.1001/jama.2020.2648.
2. Velavan P, Meyer CG. The COVID-19 epidemic. *Trop Med Int Health*. 2020;25(3):278-280. DOI: 10.1111/tmi.13383.
3. Blanco-Lobo P, Nogales A, Rodríguez L, Martínez-Sobrido L. Novel approaches for the development of live attenuated influenza vaccines. *Viruses*. 2019;11(2):190-224. DOI: 10.3390/v11020190.
4. Driggin E, Madhavan MV, Bikdeli B, Chuich T, Laracy J, Bondi-Zoccai G, et al. Cardiovascular considerations for patients, health care workers, and health systems during the coronavirus disease 2019 (COVID-19) Pandemic. *J Am Coll Cardiol*. 2020;75(18):2352-2371. DOI: 10.1016/j.jacc.2020.03.031.
5. Sigrist CJ, Bridge A, Le Mercier P. A potential role for integrins in host cell entry by SARS-CoV-2. *Antiviral Res*. 2020;177:104759,1-4. DOI: 10.1016/j.antiviral.2020.104759.
6. Wu J, Wu X, Zeng W, Guo D, Fang Z, Chen L, et al. Chest CT findings in patients with corona virus disease 2019 and its relationship with clinical features. *Invest Radiol*. 2020;55(5):257-261. DOI: 10.1097/RLI.0000000000000670.
7. Rossman H, Keshet A, Shilo S, Gavrieli A, Bauman T, Cohen O, et al. A framework for identifying regional outbreak and spread of COVID-19 from one-minute population-wide surveys. *Nat Med*. 2020;26:634-638. DOI: 10.1038/s41591-020-0857-9.
8. Tomasi D. Coronavirus disease (COVID-19), a socioepidemiological review-2. *Vermont Academy of Arts and Sciences. VAAS*. 2020;1:1-8.
9. Epidemiology working group for NCIP epidemic response, chinese center for disease control and prevention. The epidemiological characteristics of an outbreak of 2019 novel coronavirus diseases (COVID-19) in China. *Zhonghua Liu Xing Bing Xue Za Zhi*. 2020;41(2):145-151. DOI: 10.3760/cma.j.issn.0254-6450.2020.02.003.
10. Wong G, Liu W, Liu Y, Zhou B, Bi Y, Gao GF. MERS, SARS, and Ebola: the role of super-spreaders in infectious disease. *Cell Host Microbe*. 2015;18(4):398-401. DOI: 10.1016/j.chom.2015.09.013.
11. Ki M. 2015 MERS outbreak in Korea: hospital-to-hospital transmission. *Epidemiol Health*. 2015;37:e2015033,1-4. DOI: 10.4178/epih/e2015033.
12. Liu Y, Gayle AA, Wilder-Smith A, Rocklöv J. The reproductive number of COVID-19 is higher compared to SARS coronavirus. *J Travel Med*. 2020;27(2):taaa021. DOI: 10.1093/jtm/taaa021.
13. Kennedy T. Managing the drug discovery/development interface. *Drug Discov Today*. 1997;2(10):436-444. DOI: 10.1016/S1359-6446(97)01099-4.
14. Adams CP, Brantner VV. Estimating the cost of new drug development: is it really \$802 million? *Health Aff (Millwood)*. 2006;25(2):420-428. DOI: 10.1377/hlthaff.25.2.420.
15. Mullard A. New drugs cost US \$2.6 billion to develop. *Nature Rev Drug Discov*. 2014;13:877. DOI: 10.1038/nrd4507.
16. Contini A. Virtual screening of an FDA approved drugs database on two COVID-19 coronavirus proteins. *ChemRxiv*. 2020:1-6. Available in: [https://chemrxiv.org/articles/preprint/Virtual\\_Screening\\_of\\_an\\_FDA\\_Approved\\_Drugs\\_Database\\_on\\_Two\\_COVID-19\\_Coronavirus\\_Proteins/11847381](https://chemrxiv.org/articles/preprint/Virtual_Screening_of_an_FDA_Approved_Drugs_Database_on_Two_COVID-19_Coronavirus_Proteins/11847381).
17. Dayer MR. Old drugs for newly emerging viral disease, COVID-19: bioinformatic prospective. 2020;arXiv:2003.04524:116. Available in: <https://arxiv.org/abs/2003.04524>.
18. Xue H, Li J, Xie H, Wang Y. Review of drug repositioning approaches and resources. *Int J Biol Sci*. 2018;14(10):1232-1244. DOI: 10.7150/ijbs.24612.
19. Deng X, Yu X, Pei J. Regulation of interferon production as a potential strategy for COVID-19 treatment. 2020;arXiv:2003.00751:1-9. Available in: <https://arxiv.org/abs/2003.00751>.
20. Macchiagodena M, Pagliai M, Procacci P. Inhibition of the main protease 3CL-pro of the coronavirus disease 19 via structure-based ligand design and molecular modeling. 2020;arXiv:2002.09937:1-28. <https://arxiv.org/abs/2002.09937>.

21. Arya R, Das A, Prashar V, Kumar M. Potential inhibitors against papain-like protease of novel coronavirus (SARS-CoV-2) from FDA approved drugs. ChemRxiv. 2020:1-8. Available in: [https://chemrxiv.org/articles/preprint/Potential\\_Inhibitors\\_Against\\_Papainlike\\_Protease\\_of\\_Novel\\_Coronavirus\\_COVID-19\\_from\\_FDA\\_Approved\\_Drugs/11860011/2](https://chemrxiv.org/articles/preprint/Potential_Inhibitors_Against_Papainlike_Protease_of_Novel_Coronavirus_COVID-19_from_FDA_Approved_Drugs/11860011/2).
22. Hosseini FS, Amanlou M. Anti-HCV and anti-malaria agent, potential candidates to repurpose for coronavirus infection: virtual screening, molecular docking, and molecular dynamics simulation study. Life Sci. 2020;258:118205,1-14. DOI: 10.1016/j.lfs.2020.118205.
23. Haider Z, Subhani MM, Farooq MA, Ishaq M, Khalid M, Khan RSA, *et al.* *in silico* discovery of novel inhibitors against main protease (Mpro) of SARS-CoV-2 using pharmacophore and molecular docking based virtual screening from ZINC database. 2020. DOI: 10.20944/preprints202002.0431.v1.
24. Talluri S. Molecular docking and virtual screening based prediction of drugs for COVID-19. Comb Chem High Throughput Screen. 2020. DOI: 10.2174/1386207323666200814132149.2020.
25. Jin Z, Du X, Xu Y, Deng Y, Liu M, Zhao Y, *et al.* Structure-based drug design, virtual screening and high-throughput screening rapidly identify antiviral leads targeting COVID-19. Nature. 2020;582:289-293. DOI: 10.1038/s41586-020-2223-y.
26. Smith M, Smith JC. Repurposing therapeutics for COVID-19: supercomputer-based docking to the SARS-CoV-2 viral Spike protein and viral Spike protein-human ACE2 interface. ChemRxiv. 2020:1-28. Available in: [https://chemrxiv.org/articles/preprint/Repurposing\\_Therapeutics\\_for\\_the\\_Wuhan\\_Coronavirus\\_nCov-2019\\_Supercomputer-Based\\_Docking\\_to\\_the\\_Viral\\_S\\_Protein\\_and\\_Human\\_ACE2\\_Interface/11871402](https://chemrxiv.org/articles/preprint/Repurposing_Therapeutics_for_the_Wuhan_Coronavirus_nCov-2019_Supercomputer-Based_Docking_to_the_Viral_S_Protein_and_Human_ACE2_Interface/11871402).
27. Li F. Structure, function, and evolution of coronavirus Spike proteins. Annu Rev Virol. 2016;3(1):237-261. DOI: 10.1146/annurev-virology-110615-042301.
28. Bian H, Zheng ZH, Wei D, Zhang Z, Kang WZ, Hao CQ, *et al.* Meplazumab treats COVID-19 pneumonia: an open-labelled, concurrent controlled add-on clinical trial. MedRxiv. 2020:1-21. DOI: 10.1101/2020.03.21.20040691v3.
29. Kadam RU, Wilson IA. Structural basis of influenza virus fusion inhibition by the antiviral drug arbidol. Proc Natl Acad Sci U S A. 2017;114(2):206-214. DOI: 10.1073/pnas.1617020114.
30. Lung J, Lin YS, Yang YH, Chou YL, Shu LH, Cheng YC, *et al.* The potential chemical structure of anti-SARS-CoV-2 RNA-dependent RNA polymerase. J Med Virol. 2020;92(6):693-697. DOI: 10.1002/jmv.25761.
31. Mirza MU, Froeyen M. Structural elucidation of SARS-CoV-2 vital proteins: computational methods reveal potential drug candidates against main protease, Nsp12 RNA-dependent RNA polymerase and Nsp13 helicase. J Pharm Anal. 2020;10(4):320-328. DOI: 10.1016/j.jpha.2020.04.008.
32. Zhang H, Penninger JM, Li Y, Zhong N, Slutsky AS. Angiotensin-converting enzyme 2 (ACE2) as a SARS-CoV-2 receptor: molecular mechanisms and potential therapeutic target. Intensive Care Medicine. 2020:1-5.
33. Hoffmann M, Kleine-Weber H, Schroeder S, Krüger N, Herrler T, Erichsen S, *et al.* SARS-CoV-2 cell entry depends on ACE2 and TMPRSS2 and is blocked by a clinically proven protease inhibitor. Cell. 2020;181(2):271-280.e8. DOI: 10.1016/j.cell.2020.02.052.
34. Prajapat M, Shekhar N, Sarma P, Avti P, Singh S, Kaur H, *et al.* Virtual screening and molecular dynamics study of approved drugs as inhibitors of Spike protein S1 domain and ACE2 interaction in SARS-CoV-2. J Mol Graph Model. 2020;101:107716,1-13. DOI: 10.1016/j.jmgm.2020.107716.
35. Andersen KG, Rambaut A, Lipkin WI, Holmes EC, Garry RF. The proximal origin of SARS-CoV-2. Nat Med. 2020;26(4):450-452. DOI: 10.1038/s41591-020-0820-9.
36. Wrapp D, Wang N, Corbett KS, Goldsmith JA, Hsieh CL, Abiona O, *et al.* Cryo-EM structure of the 2019-nCoV Spike in the prefusion conformation. Science. 2020;367(6483):1260-1263. DOI: 10.1126/science.abb2507.
37. Rocco A, Compare D, Coccoli P, Esposito C, Di Spirito A, Barbato A, *et al.* Vitamin B12 supplementation improves rates of sustained viral response in patients chronically infected with hepatitis C virus. Gut. 2013;62(5):766-773. DOI: 10.1136/gutjnl-2012-302344.
38. Paltiel O, Falutz J, Veilleux M, Rosenblatt DS, Gordon K. Clinical correlates of subnormal vitamin B12 levels in patients infected with the human immunodeficiency virus. Am J Hematol. 1995;49(4):318-322. DOI: 10.1002/ajh.2830490410.
39. Kaushik N, Anang S, Ganti KP, Surjit M. Zinc: a potential antiviral against hepatitis E virus infection? DNA Cell Biol. 2018;37(7):593-599. DOI: 10.1089/dna.2018.4175.
40. Read SA, Parnell G, Booth D, Douglas MW, George J, Ahlenstiel G. The antiviral role of zinc and metallothioneins in hepatitis C infection. J Viral Hepat. 2018;25(5):491-501. DOI: 10.1111/jvh.12845.